HORIZON EUROPE PROGRAMME
HORIZON-CL4-2023-DIGITAL-EMERGING-01-33

GA No. 101135196

Developing New 2D Materials and Heterostructures for Printed Digital Devices

2D-PRINTABLE - Deliverable report

D5.2. – Flake to flake contacts improvement

Funded by
the European Union

Deliverable No.	D5.2	
Related WP	WP5	
Deliverable Title	Flake to flake contacts improvement	
Deliverable Date	23/06/2025	
Deliverable Type	REPORT	
Dissemination level	Public (PU)	
Author(s)	Jonathan Coleman (TCD) Cian Gabbett (TCD) Georg Duesberg (UniBwM)	11/06/2025 23/06/2025 24.06.2025
Checked by	Georg Duesberg (UniBwM)	2025.06.2025
Reviewed by	Paolo Samori (UNISTRA) Francesco Bonaccorso (BeD)	2025-06-26 2025-06-27
Approved by	Jonathan Coleman (TCD) - Project Coordinator	2025-06-27
Status	Final	2025-06-27

Document History

Version	Date	Editing done by	Remarks
V1.0	11/06/2025	Jonathan Coleman	
V1.1	18/06/2025	Cian Gabbett	
V2.0	27/06/2025	Georg Duesberg	
FINAL			

Project Scientific Abstract

The 2D-PRINTABLE project aims to integrate sustainable large-scale liquid exfoliation techniques with theoretical modelling to efficiently produce a wide range of new 2D materials (2DMs), including conducting, semiconducting, and insulating nanosheets. The focus includes developing the printing and liquid phase deposition methods required to fabricate networks and multicomponent heterostructures, featuring layer-by-layer assembly of nanometre-thick 2DMs into ordered multilayers. The goal is to optimize these printed networks and heterostructures for digital systems, unlocking new properties and functionalities. The project also seeks to demonstrate various printed digital devices, including proof-of-principle, first-time demonstration of all-printed, all-nanosheet, heterostack light-emitting diodes (LEDs). In conclusion, 2D-PRINTABLE will prove 2D materials to be an indispensable material class in the field of printed electronics, capable of producing far-beyond-state-of-the-art devices that can act as a platform for the next generation of printed digital applications.

Public summary

This report presents a detailed investigation into improving flake-to-flake contacts in printed two-dimensional material (2DM) networks, a critical bottleneck in enabling high-performance printed electronics. When nanosheets are deposited into a network, the electrical resistance at the junctions between flakes (R_J) can significantly exceed the resistance across individual nanosheets (R_{NS}), severely limiting the overall network mobility (μ_{Net}). To address this, Deliverable 5.2 develops and applies advanced methodologies to independently measure R_J and R_{NS} using a combination of AC impedance spectroscopy and DC electrical measurements. This allows for the development of charge transport models and a quantitative assessment of junction-dominated conduction.

Initial experiments using networks of electrochemically exfoliated (EE) graphene and MoS_2 nanosheets reveal that R_J dominates in standard printed films, leading to mobilities far below the intrinsic nanosheet value. A key finding is that R_J strongly depends on the lateral dimensions of the nanosheets, where larger area flakes form larger, more conformal junctions that reduce R_J significantly. Guided by this insight, size-selected monolayer MoS_2 nanosheet inks were produced using liquid cascade centrifugation and deposited into highly aligned films via liquid-liquid interfacial deposition (LLID). These networks exhibited junction resistances below R_{NS}, achieving mobilities up to 30 $cm^2 (Vs)^{-1}$, which approaches the intrinsic limit of the EE MoS_2 nanosheets (~40 $cm^2 (Vs)^{-1}$) as measured by terahertz spectroscopy.

This work demonstrates a successful strategy for fabricating printed 2DM networks with hugely improved flake-to-flake contacts, where the network mobility closely approaches the nanosheet mobility. It provides a clear framework for further engineering of printed heterostructures and aligns directly with several key objectives of the 2D-PRINTABLE project, particularly those targeting improved electrical performance in all-nanosheet printed devices.

Contents

List of Figures

Abbreviations & Definitions

Abbreviation	Explanation
2DM	Two-dimensional material
R_J	Junction resistance
R_{NS}	Nanosheet resistance
μ_{Net}	Network mobility
μ_{NS}	Nanosheet mobility
AFM	Atomic force microscopy
SEM	Scanning electron microscopy
TEM	Transmission electron microscopy
EE	Electrochemical exfoliation
LLID	Liquid-liquid interfacial deposition
TFT	Thin film transistor
DMF	Dimethylformamide
IPA	Isopropanol
ρ_{Net}	Network resistivity

1 Introduction

This report outlines the progress made improving the flake-to-flake contacts in printed two-dimensional material (2DM) networks, which leads to enhanced charge transport and network performance. Junction-limited 2DM networks can be classed as those where the inter-nanosheet junction resistance, R_J, is greater than the intrinsic resistance of the constituent nanosheets, R_{NS}, such that $R_J > R_{NS}$. This leads to heavily reduced carrier mobilities in printed 2DM networks, μ_{Net}, when compared to the intrinsic nanosheet mobility, μ_{NS}. Thus, realising high performance printed devices requires improvement of the flake-to-flake contacts to minimise this junction resistance relative to the nanosheet resistance. Strategies to achieve this include optimising the nanosheet dimensions (D3.1) or techniques used to deposit them as investigated in WP3 (D3.3), as well as chemical cross-linking, which is a key objective of WP2. However, without the ability to measure R_J and R_{NS}, assessing the progress of various strategies towards achieving $R_J < R_{NS}$ is difficult.

In this deliverable report, we will describe methods to measure both R_J and R_{NS} for both semiconducting and conducting nanosheets using both DC and AC electrical measurements on their networks. This builds upon the work of D4.1. Using spray-coated films of electrochemically exfoliated (EE) graphene nanosheets, the factors that influence R_J at flake-to-flake contacts, including nanosheet area and thickness have been studied. Here, networks of thinner, larger nanosheets demonstrated improved performance and reduced junction resistances. By then combining these findings with tailored deposition strategies, such as liquid-liquid interfacial deposition (LLID) (D3.3), highly aligned networks of EE MoS_2 nanosheets with large area junctions were produced. Electrical measurements on these optimised networks found the 2DMs to have carrier mobilities very close to the limiting mobility of their individual nanosheets, where $\mu_{Net} \sim 0.75 \times \mu_{NS}$. In summary, the work presented in this report provides a working strategy for producing high mobility networks with improved flake-to-flake contacts.

2 Methods

2.1 Background

As part of Deliverable 5.2, the nature of flake-to-flake contacts between nanosheets in printed 2DM networks were studied. The quality of these inter-nanosheet contacts determines how efficiently charges can traverse these networks and represent a fundamental barrier to producing 2DM films and devices that capitalise on the superlative properties of their constituent nanosheets. Optimising the flake-to-flake contacts involves careful consideration of the nanosheets themselves, as well the morphology and electrical properties of the ensemble when these nanosheets are deposited into a 2DM film or device. A range of microscopic techniques were used to characterise the nanosheet dimensions and network morphologies, including but not limited to atomic force microscopy (AFM), scanning electron microscopy (SEM) and transmission electron microscopy (TEM). Before the nanosheet junctions can be optimised, it was necessary to develop methods to measure the junction resistance, R_J. Here, we used impedance spectroscopy in tandem with simple models to extract the nanosheet resistance, R_{NS}, and R_J from printed electrochemically exfoliated (EE) MoS_2 films. To determine the role of nanosheet size on the interflake contacts, DC electrical measurements of the network resistivity as a function of nanosheet area (determined from AFM) were performed on networks of EE graphene nanosheets. Finally, the learnings from D5.2 were applied to deposit EE MoS_2 films with optimised flake-to-flake contacts. MoS_2 monolayers were produced using electrochemical exfoliation and liquid cascade centrifugation.[1] These were then deposited into highly-aligned networks with large-area junctions using liquid-liquid interfacial deposition (LLID). The network structure was characterised using AFM, TEM, and SEM, while the film mobilities were determined using thin-film transistor (TFT) measurements.

2.2 Procedures

Graphene and MoS_2 inks were produced using established EE protocols as described in D3.1.[2] Following exfoliation, the 2DM inks were size-selected using liquid cascade centrifugation to remove unexfoliated material and ensure uniform flake size distributions.[1] Following this the EE graphene and MoS_2 inks were transferred from dimethylformamide (DMF) to isopropanol (IPA) using centrifugation for printing. AFM was used to measure the nanosheet length, width, area (length × width) and thickness for both the EE graphene and MoS_2.

EE MoS_2 inks were deposited into nanosheet films using LLID as described in D3.1.[3] The networks were deposited onto Ti:Au (5 nm:50 nm) evaporated bottom contacts in an interdigitated electrode (IDE) geometry for electrical characterisation. The network resistivity was first measured using DC electrical measurements on a Janis ST-500 probe station. Following this, the AC response of the networks was measured using impedance spectroscopy (Keysight E4990E analyser) developed as part of WP5. Here, both the nanosheet resistance, R_{NS}, and junction resistance, R_J, in the networks were measured and extracted using simple models developed as part of WP4 & WP5.[2]

The surface coverage and layer thickness of the LLID EE MoS_2 films was determined using AFM, while the nature of the flake-to-flake contacts was characterised using cross-sectional TEM. TFT measurements were used to calculate the network mobilities. Bottom contact, dielectrically gated EE MoS_2 TFTs were fabricated using LLID EE MoS_2 on n-doped silicon substrates with a 230 nm SiO_2 gate oxide. Electronic testing of all MoS_2 TFTs was performed using a Janis ST-500 probe station in conjunction with a Keithley 4200A-SCS parameter analyzer.

EE graphene inks were patterned into films using spray-coating through stainless steel shadow masks. DC electrical measurements of the network resistivity were performed in a 4-point probe configuration using an electrical probe station and a source meter (Keithley KE2612A).

2.3 Data Analysis

Data analysis was performed using specialised software specific to each technique as needed. This includes Gwyddion 2.61 for AFM measurements, ImageJ for SEM and TEM image analysis, and OriginPro for generalised numerical data analysis, production of graphs and curve fitting.

3 Results & Discussion

3.1 Measuring R_{NS} and R_J in Printed 2DM Networks

Before R_J and R_{NS} can be measured, a model that leads to an equation for the resistivity of a network of 2D nanosheets, ρ_{Net}, was developed.[2] This model is based on analysis of chains of resistors and leads to the equation

$$\rho_{Net} \approx \frac{\left[\rho_{NS} + 2t_{NS}R_J\right]}{\left(1 - P_{Net}\right)} \qquad (1)$$

where t_{NS} is the nanosheet thickness, R_J is the junction resistance, ρ_{NS} is the nanosheet resistivity and P_{Net} is the network porosity. Extensive preliminary measurements showed that this equation matches experimental data for electrical resistivity in printed nanosheet networks.[2]

Next, this equation was combined with impedance spectroscopy to develop a method for directly measuring R_J from a printed 2DM network. To extract absolute values for R_{NS} and R_J in nanosheet networks, the impedance spectra of the network (Z_{Net}) must be converted to spectra representing the average nanosheet-junction pair ($Z_{NS\text{-}J}$) within the network. These nanosheet-junction (NS-J) spectra can then be analysed based on microscopic considerations. Eqn. 1 is derived from an equation that relates the DC resistivity of a nanosheet network, ρ_{Net}, to the resistance of the average nanosheet-junction pair, $(R_{NS} + R_J)$. We propose that the same scaling exists between the complex resistivity of the network, ρ^*_{Net}, and $Z_{NS\text{-}J}$. This yields an equation that converts the real and imaginary parts of the network impedance, Z_{Net}, to those representing the average nanosheet-junction pair, once P_{Net}, t_{NS}, as well as the channel area, A, and length, L, are known

$$Z_{NS\text{-}J} = Z_{Net}\frac{A}{L}\frac{(1 - P_{Net})}{2t_{NS}} \qquad (2)$$

The real (Re) part of the complex impedance was measured as a function of frequency for a network of electrochemically exfoliated (EE) MoS_2 deposited using liquid-liquid interfacial deposition (LLID) (Fig. 1a). Then, Eqn. 2 can be used to convert the network impedance, Z_{Net}, into the impedance of the average nanosheet-junction pair, $Z_{NS\text{-}J}$. The real component of $Z_{NS\text{-}J}$ is shown in Fig. 1b, and the next step is to fit this data.

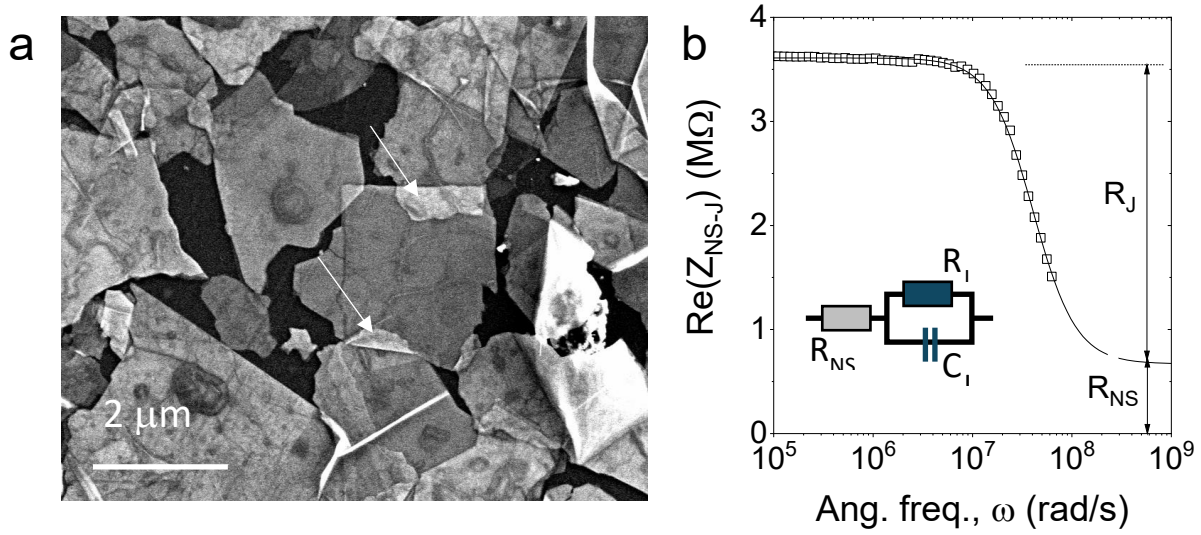

Figure 1: Extracting R_J and R_{NS} from liquid-liquid interfacially deposited networks of EE MoS_2. a) SEM image of a network of a LLID EE MoS_2 nanosheets with junctions shown by arrows. **b)** Real impedance spectrum of an (average) nanosheet junction pair. The solid line is a fit to an equivalent circuit model that allows one to extract the nanosheet, R_{NS}, and junction, R_J, resistances. Inset: An equivalent Randles circuit representing a nanosheet-junction pair.

In the AC domain, the nanosheet-junction pair can be described as the nanosheet resistance, R_{NS}, in series with a parallel resistor, R_J, and capacitor, C_J, representing the junction (Fig. 1b, inset), an arrangement referred to as the Randles circuit. We chose to fit to the Re(Z_{NS-J}) spectrum as the extracted parameters have a higher accuracy compared to fitting other spectra. Such spectra can be fitted using equations appropriate to the Randles circuit to yield values of R_{NS}, R_J, and C_J. We account for the distribution of junction resistances by fitting the data using a modified equation for the Randles circuit

$$\mathrm{Re}\,Z_{\mathrm{NS\text{-}J}}(\omega) = R_{\mathrm{NS}} + \frac{R_{\mathrm{J}}\left[1+(\omega R_{\mathrm{J}}C_{\mathrm{J}})^{\mathrm{n}}\cos(n\pi/2)\right]}{1+2(\omega R_{\mathrm{J}}C_{\mathrm{J}})^{\mathrm{n}}\cos(n\pi/2)+(\omega R_{\mathrm{J}}C_{\mathrm{J}})^{2\mathrm{n}}} \qquad (3)$$

where n is an ideality factor that decreases from 1 as the distribution of (R_JC_J) values in the network broadens. We find excellent fits, yielding values of R_J = (2.9 ± 0.1) MΩ, R_{NS} = (0.67 ± 0.07) MΩ, C_J = (8.4 ± 0.4) ×10^{-15} F, and n ≈ 0.985. Over five devices on the same substrate, R_{NS} typically varies by <20% with R_J and C_J showing larger spreads (with a std. dev./mean of <60%) due to spatial morphology variations. This measurement clearly shows that networks of EE MoS_2 nanosheets have $R_J > R_{NS}$ such that junctions limit charge transport. This is expected to lead to network mobilities which are lower than those of the

nanosheets themselves (i.e. $\mu_{\mathrm{Net}} < \mu_{\mathrm{NS}}$). To confirm this, we performed transistor measurements on these networks finding mobilities of $\mu_{\mathrm{Net}} \sim 7$ cm^2 (Vs)$^{-1}$.

In addition, we performed terahertz spectroscopy to measure the mobility of the nanosheets themselves finding $\mu_{\mathrm{NS}} = 40$ cm^2 (Vs)$^{-1}$, which confirms that the presence of junctions in these systems significantly reduces the network mobility. This highlights the importance of developing a strategy for reducing the junction resistance to the point where $R_J < R_{NS}$.

3.2 The Influence of Nanosheet Dimensions on R_J in Printed 2DM Networks

To achieve this reduction in R_J, it was necessary to understand the factors that control the junction resistance. This was investigated using electrochemically exfoliated graphene as a model system. The EE graphene nanosheet inks were size-selected using a process known as liquid cascade centrifugation[1]. This resulted in six fractions, each containing nanosheets with different sizes. For all fractions, we performed AFM to measure the distribution of nanosheet lengths, l_{NS}, widths, w_{NS}, and thicknesses, t_{NS}. As predicted by simple models[4] for each fraction we found the nanosheet length, width and thickness to be mutually proportional such that we can define roughly constant aspect ratios relating the nanosheet length, width, and thickness as: $k_{lt} = l_{NS} / t_{NS}$, $k_{wt} = w_{NS} / t_{NS}$ and $k_{\mathrm{lw}} = l_{\mathrm{NS}} / w_{\mathrm{NS}}$. Spray coating was used to print networks for each graphene nanosheet size and the network resistivity, ρ_{Net}, is plotted versus mean nanosheet thickness, $\langle t_{NS} \rangle$ in Fig. 2a.

It is clear from this data that the network resistivity decreases with nanosheet thickness, behavior which is inconsistent with the prediction of Eqn. 1. The reason for this is that Eqn. 1 assumes that the junction resistance is independent of nanosheet size. However, the conformal, large area junctions achieved in networks of high aspect ratio EE nanosheets almost certainly depend on nanosheet size. We assume that large area junctions have junction resistances that scale with junction area, and that this junction area is directly proportional to nanosheet area. Utilising the aspect ratios defined above and assuming that the junction area is a fixed fraction (f_{J}) of the nanosheet area, yields the following equation for network resistivity

$$\rho_{Net} \approx \frac{1}{(1-P_{Net})}\left[\rho_{NS} + \frac{2(RA)_J}{f_J k_{lt} k_{wt}} \frac{1}{t_{NS}}\right] \qquad (4)$$

where $(RA)_J$ is a parameter describing intersheet charge transport. Crucially, Eqn. 4 has a different nanosheet size scaling to Eqn. 1 and predicts that ρ_{Net} scales linearly with $1/t_{NS}$.

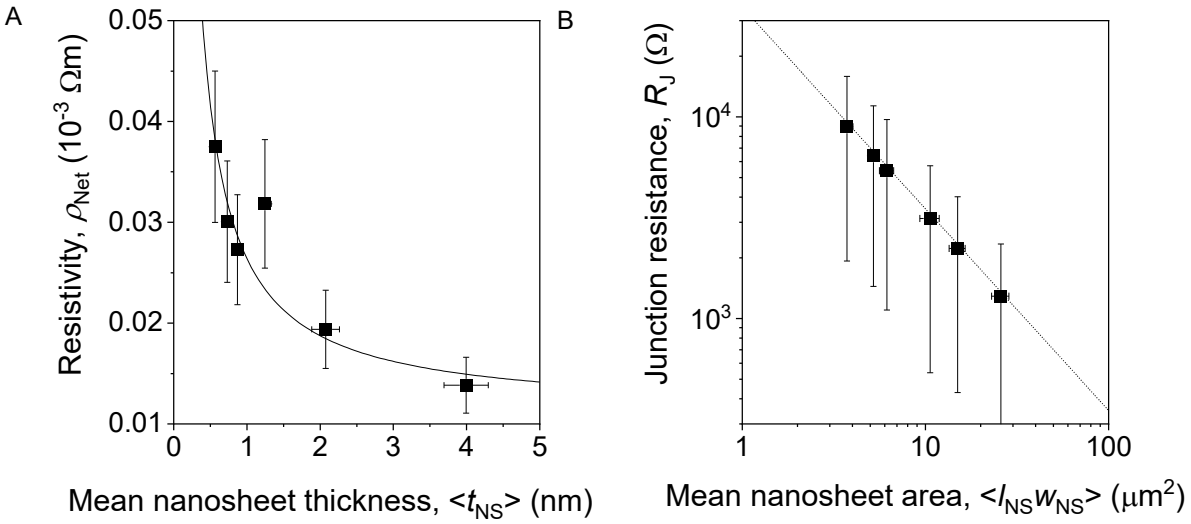

Figure 2: Influence of Nanosheet Dimensions on ρ_{Net} and R_J in Printed EE Graphene Networks. a) Resistivity of printed networks of electrochemically exfoliated graphene nanosheets, ρ_{Net}, plotted versus mean nanosheet thickness, <t_{NS}>. The solid line is a fit to Eqn. 4. **b)** Extracted junction resistance, R_J, plotted as a function of the average nanosheet area, $A_{NS} = l_{NS}w_{NS}$.

We fit our data in Fig. 2a with Eqn. 4, finding very good agreement. Combining the fit parameters with measured values for P_{Net} = 0.02, k_{lt} = 2,633 and k_{wt} = 1,771 will allow us to obtain ρ_{NS} and $(RA)_J$, once f_J is known. Previously, we have measured f_J in networks of EE MoS_2 using SEM imaging, finding values of 0.33,[5] and 0.4.[2] Assuming EE graphene behaves similarly, we can estimate f_J = 0.37 ± 0.03. This allows us to calculate ρ_{NS} = (1.0 ± 0.3) × 10^{-5} Ω m and $(RA)_J$ = (1.2 ± 0.8) × 10^{-8} Ω m^2. Using this information, we can calculate the junction resistance for different nanosheet areas as shown in Fig. 2b. This work clearly shows that the junction resistance can be dramatically reduced by increasing the nanosheet area (or lateral size), $A_{NS} = l_{NS}w_{NS}$.

3.3 Engineering Printed 2DM Networks with Reduced R_J and Enhanced Mobility

Thus far, we have seen that carrier mobility, μ_{Net}, in printed 2DM networks is heavily reduced when compared to the mobility of their intrinsic nanosheets, μ_{NS}, due to junction resistances that exceed the nanosheet resistance (i.e. $R_J > R_{NS}$). Work undertaken in this deliverable has shown that both R_J and R_{NS} can now be measured using impedance spectroscopy (Fig. 1), and that large aspect ratio nanosheets

can lead to reductions in R_J and the network resistivity, ρ_{Net} (Fig. 2). To build upon this, protocols to deposit conformal and highly aligned networks of high aspect ratio EE nanosheets were developed with a view to enhancing the network mobility. By rearranging Eqn. 1 it can be shown that it should be possible to produce networks with mobility approaching that of the nanosheets themselves so long as $R_J << R_{NS}$.

$$\frac{\rho_{Net}}{\rho_{NS}} \approx \left[1 + \frac{R_J}{R_{NS}}\right] = \frac{\mu_{NS}}{\mu_{Net}} \qquad (5)$$

Eqn. 5 implies that in addition to the junction resistance being small, we want the nanosheet resistance to be large. The nanosheet resistance is given by $R_{NS} = \rho_{NS} / 2t_{NS}$.[6] This clearly shows that the nanosheet resistance can be increased by minimizing the nanosheet thickness. Combined with the data in Fig. 2b and Eqn. 5, this suggests that to maximize network mobility, the nanosheet area should be maximised and the nanosheet thickness minimised. In other words, large area monolayers are required.

To investigate this, large area monolayers of MoS_2 were produced and deposited into highly aligned films with large area junctions. The MoS_2 nanosheets were created using electrochemical exfoliation, which is known to give large, thin nanosheets. We then centrifuged the resultant nanosheet dispersion in a manner known to remove all nanosheets except the monolayers. This resulted in an ink consisting of almost exclusively monolayers with reasonably large areas.[3] These nanosheets were deposited using liquid-liquid interfacial deposition (LLID) to produce a highly aligned single layer of these nanosheets as shown in Fig. 3a. We then performed multiple depositions to build up layers stacked on top of each other as shown schematically in Fig. 3b. It was confirmed that the resulting films consisted of very highly aligned nanosheets using cross-sectional TEM (Fig. 3c). We note that these films should meet all the criteria required to achieve high mobility - the nanosheets are highly aligned leading to large area junctions, while the nanosheet thickness is minimized and the nanosheet area as is as large as we could achieve.

Field effect transistor measurements were performed on the resultant films to measure their carrier mobility. An example of such a transfer curve is shown in Fig. 3d. The resulting curves were corrected for contact resistance using the *Y*-function method and the network mobility was extracted. The resultant network mobility, μ_{Net}, is plotted as a function of network thickness (layer number) in Fig. 3e.

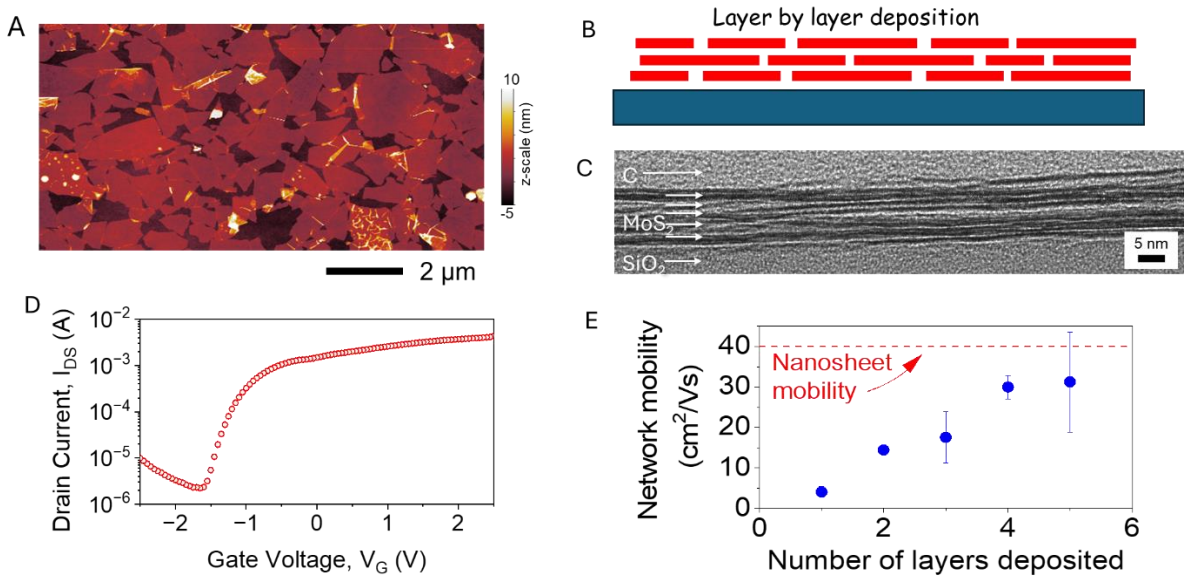

Figure 3: High Mobility EE MoS_2 Networks with Engineered Conformal Junctions. a) AFM image of a single layer (1L) of LLID EE MoS_2 monolayers. **b)** Schematic showing layer by layer deposition of such layers. **c)** TEM cross-section of a multilayer LLID EE MoS_2 network. **d)** Representative transfer curve, measured on a multilayer EE MoS_2 TFT, used to extract mobility. **e)** Contact resistance corrected network mobility, μ_{Net}, as a function of layer number. The dashed line illustrates the nanosheet mobility, μ_{NS}, as measured by terahertz spectroscopy.

The network mobility, μ_{Net}, is clearly seen to increase with deposition layer number in Fig. 3e, saturating at ~ 30 cm^2 $(Vs)^{-1}$ for a 5-layer device. That is just short of the intrinsic mobility of the nanosheets themselves, μ_{NS}, which was measured using terahertz spectroscopy to be 40 cm^2 $(Vs)^{-1}$. Detailed analysis showed the junction resistance to be less than the nanosheet resistance for these networks, consistent with values of $R_J / R_{NS} \sim 0.2$. This demonstrates that our strategy of minimizing nanosheet thickness while maximizing nanosheet area, while also optimising the deposition technique, was successful in minimizing R_J. This resulted in network mobilities that approached those of the nanosheets themselves for LLID networks of EE MoS_2 nanosheets.

3.4 Contribution to project (linked) Objectives

By developing methods to both quantify and optimise flake-to-flake contacts in printed 2DM networks, the results presented in this deliverable offer a roadmap to reduce R_J to the point that the network mobilities begin to approach the intrinsic mobility of their constituent nanosheets. This represents a significant contribution to the overall objective of 2D-PRINTABLE. More specifically, the work in D5.2 contributes to O4.2: Establish basic and advanced characterization of nanosheet networks and heterostructures to assess morphology and nanosheet coupling and O5.2: Characterization and optimization of charge transport in printed networks and flake-level homostructures. Furthermore, the results in this deliverable are currently informing work towards achieving both O5.3: Characterization and optimization of charge injection and transport in printed heterostructures and O6.1: TFTs with charge carrier mobilities for both p- and n-type exceeding 100 $cm^2 (Vs)^{-1}$.

3.5 Contribution to major project exploitable result

Not applicable.

4 Conclusion and Recommendation

In summary, a method to optimise the mobility of printed nanosheet networks by improving the flake-to-flake contacts has been developed as part of Deliverable 5.2. It has been shown using impedance spectroscopy that by using standard processing techniques, these networks display junction resistances that are significantly higher than the resistances of the nanosheets themselves.[2] This results in network mobilities considerably lower than those of the individual nanosheets (i.e. $\mu_{Net} < \mu_{NS}$). Studies to identify the factors controlling the junction resistance at flake-to-flake contacts were then performed. It has been shown that the junction resistance scales with nanosheet area in such a way that large area nanosheets should lead to low resistance junctions. In addition, we found that the nanosheet resistance can be increased by reducing the nanosheet thickness. Taken together, this predicts that very high mobilities might be achieved using monolayer nanosheets with large area. We tested this hypothesis by producing inks containing only monolayer MoS_2 nanosheets of reasonably large area. These were fabricated into highly aligned networks with large area junctions using an optimised liquid-liquid interfacial deposition process. This was found to result in nanosheet networks with carrier mobilities very close to the limiting mobility of the individual nanosheets.[3] We believe that we have demonstrated a working strategy for producing high mobility networks with improved flake-to-flake contacts. Our next step is to apply this strategy to networks of nanosheets with high intrinsic mobility, which have been identified from computational studies as part of WP1.

5 Risks and interconnections

5.1 Risks/problems encountered

Risk No.	What is the risk	Probability of risk occurrence[1]	Effect of risk[1]	Solutions to overcome the risk

[1)] Probability risk will occur: 1 = high, 2 = medium, 3 = Low

5.2 Interconnections with other deliverables

Deliverable 5.2 is linked with many other deliverables in the 2D PRINTABLE project. It builds upon the work D3.1 “Ink production & printing” and D4.1 “Characterisation of nanosheets, networks and heterostacks built from initially available 2D materials”. The developments made in D5.2 will contribute to the upcoming deliverables; D4.4 “Characterisation of networks and heterostructures”, D5.3 “Electrical characterisation of films and vertical heterostructures” and D6.1 “Beyond-state-of-the-art all-nanosheet TFTs”.

6 References

1 Backes, C. *et al.* Production of Highly Monolayer Enriched Dispersions of Liquid-Exfoliated Nanosheets by Liquid Cascade Centrifugation. *ACS Nano* **10**, 1589-1601, doi:10.1021/acsnano.5b07228 (2016).

2 Gabbett, C. *et al.* Understanding how junction resistances impact the conduction mechanism in nano-networks. *Nature Communications* **15**, doi:10.1038/s41467-024-48614-5 (2024).

3 Neilson, J. *et al.* Production of Ultrathin and High-Quality Nanosheet Networks via Layer-by-Layer Assembly at Liquid–Liquid Interfaces. *ACS Nano* **18**, 32589-32601, doi:10.1021/acsnano.4c09745 (2024).

4 Backes, C. *et al.* Equipartition of Energy Defines the Size–Thickness Relationship in Liquid-Exfoliated Nanosheets. *ACS Nano* **13**, 7050-7061, doi:10.1021/acsnano.9b02234 (2019).

5 Caffrey, E. *et al.* Using Electrical Impedance Spectroscopy to Separately Quantify the Effect of Strain on Nanosheet and Junction Resistance in Printed Nanosheet Networks. *Small* **n/a**, 2406864, doi:https://doi.org/10.1002/smll.202406864 (2024).

6 Kelly, A. G., O'Suilleabhain, D., Gabbett, C. & Coleman, J. N. The electrical conductivity of solution-processed nanosheet networks. *Nature Reviews Materials* **7**, 217-234, doi:10.1038/s41578-021-00386-w (2021).

7 Acknowledgement

The author(s) would like to thank the partners in the project for their valuable comments on previous drafts and for performing the review.

Project partners:

#	Partner short name	Partner Full Name
1	TCD	TCD THE PROVOST, FELLOWS, FOUNDATION SCHOLARS & THE OTHER MEMBERS OF BOARD, OF THE COLLEGE OF THE HOLY & UNDIVIDED TRINITY OF QUEEN ELIZABETH NEAR DUBLIN
2	UNISTRA	UNIVERSITE DE STRASBOURG
3	UKa	UNIVERSITAET KASSEL
4	BED	BEDIMENSIONAL SPA
5	TUD	TECHNISCHE UNIVERSITAET DRESDEN
6	VSCHT	VYSOKA SKOLA CHEMICKO-TECHNOLOGICKA V PRAZE
7	UNR	UNIRESEARCH BV
8	UniBw M	UNIVERSITAET DER BUNDESWEHR MUENCHEN
9	EPFL	ECOLE POLYTECHNIQUE FEDERALE DE LAUSANNE

Disclaimer/ Acknowledgment

This project has received funding from the European Union's Horizon Europe research and innovation programme under grant agreement No 101135196. Views and opinions expressed are however those of the author(s) only and do not necessarily reflect those of the European Union. Neither the European Union nor the granting authority can be held responsible for them.

8 Appendix A - Quality Assurance Review Form

The following questions should be answered by all reviewers (WP Leader, reviewer, Project Coordinator) as part of the Quality Assurance procedure. Questions answered with NO should be motivated. The deliverable author will update the draft based on the comments. When all reviewers have answered all questions with YES, only then can the Deliverable be submitted to the EC.

NOTE: This Quality Assurance form will be removed from Deliverables with dissemination level "Public" before publication.

Question	**WP Leader**	**Reviewer**	**Project Coordinator**
	Georg Duesberg (UniBwM)	Paolo Samori (UNISTRA)	Jonathan Coleman (TCD)
1. *Do you accept this Deliverable as it is?*	Yes	Yes	Yes
2. *Is the Deliverable complete?* - *All required chapters?* - *Use of relevant templates?*	Yes	Yes	Yes
3. *Does the Deliverable correspond to the DoA?* - *All relevant actions preformed and reported?*	Yes	Yes	Yes
4. *Is the Deliverable in line with the 2D-PRINTABLE objectives?* - *WP objectives* - *Task Objectives*	Yes	Yes	Yes
5. *Is the technical quality sufficient?* - *Inputs and assumptions correct/clear?* - *Data, calculations, and motivations correct/clear?* - *Outputs and conclusions correct/clear?*	Yes	Yes	Yes
6. *Is created and potential IP identified and are protection measures in place?*	Yes	Yes	Yes
7. *Is the Risk Procedure followed and reported?*	Yes	Yes	Yes
8. *Is the reporting quality sufficient?* - *Clear language* - *Clear argumentation* - *Consistency* - *Structure*	Yes	Yes	Yes